

Appendix V

ANALYTICAL-EQUATION DERIVATION OF THE PHOTON ELECTRIC AND MAGNETIC FIELDS

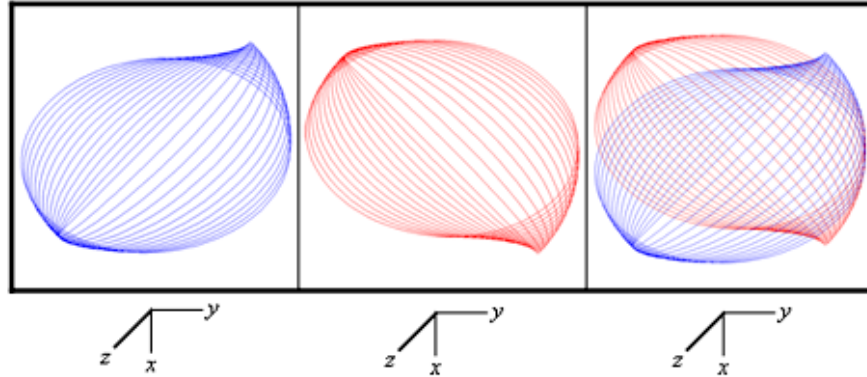
ANALYTICAL EQUATIONS TO GENERATE THE RIGHT-HANDED CIRCULARLY POLARIZED PHOTON ELECTRIC AND MAGNETIC VECTOR FIELD BY ROTATION OF THE GREAT-CIRCLE BASIS ELEMENTS ABOUT THE $(\mathbf{i}_x, \mathbf{i}_y, 0\mathbf{i}_z)$ - AXIS BY $\frac{\pi}{2}$

The right-handed circularly polarized (RHCP) photon electric and magnetic vector field (photon-e&mvf) is also generated following a similar procedure as that used to generate the orbitsphere in the Orbitsphere Equation of Motion for $\ell = 0$ Based on the Current Vector Field (CVF) section using the rotational matrices given therein. The RHCP photon-e&mvf is generated by the rotation of the basis elements comprising the great circle magnetic field line in the xz-plane and the great circle electric field line in the yz-plane about the $(\mathbf{i}_x, \mathbf{i}_y, 0\mathbf{i}_z)$ -axis by $\frac{\pi}{2}$. A first transformation matrix is generated by the combined rotation of the great circles about the z-axis by $\frac{\pi}{4}$ then about the x-axis by θ where positive rotations about an axis are defined as clockwise:

$$\begin{bmatrix} x' \\ y' \\ z' \end{bmatrix} = \begin{bmatrix} \cos\left(\frac{\pi}{4}\right) & \sin\left(\frac{\pi}{4}\right) & 0 \\ -\sin\left(\frac{\pi}{4}\right)\cos\theta & \cos\left(\frac{\pi}{4}\right)\cos\theta & \sin\theta \\ \sin\left(\frac{\pi}{4}\right)\sin\theta & -\cos\left(\frac{\pi}{4}\right)\sin\theta & \cos\theta \end{bmatrix} \cdot \left(\begin{bmatrix} 0 \\ r_n \cos\phi \\ r_n \sin\phi \end{bmatrix}_{\text{Red}} + \begin{bmatrix} r_n \cos\phi \\ 0 \\ r_n \sin\phi \end{bmatrix}_{\text{Blue}} \right) \quad (1)$$

The transformation matrix about $(\mathbf{i}_x, \mathbf{i}_y, 0\mathbf{i}_z)$ is given by multiplication of the output of the matrix given by Eq. (1) by the matrix corresponding to a rotation about the z-axis of $-\frac{\pi}{4}$. The output of the matrix given by Eq. (1) is shown in Figure AV.1 wherein θ is varied from 0 to $\frac{\pi}{2}$.

Figure AV.1. The electric, magnetic, and combined field-line pattern given by Eq. (1) from perspective of looking along the z-axis corresponding to the first great circle magnetic field line and the second great circle electric field line shown with 6 degree increments of the angle θ . (Electric field lines red; Magnetic field lines blue).



The rotation matrix about the z-axis by $-\frac{\pi}{4}$, $R_z\left(-\frac{\pi}{4}\right)$, is given by

$$R_z\left(-\frac{\pi}{4}\right) = \begin{bmatrix} \cos\left(\frac{\pi}{4}\right) & -\sin\left(\frac{\pi}{4}\right) & 0 \\ \sin\left(\frac{\pi}{4}\right) & \cos\left(\frac{\pi}{4}\right) & 0 \\ 0 & 0 & 1 \end{bmatrix} \quad (2)$$

Thus,

$$\begin{bmatrix} x' \\ y' \\ z' \end{bmatrix} = R_z\left(-\frac{\pi}{4}\right) \cdot \begin{bmatrix} \cos\left(\frac{\pi}{4}\right) & \sin\left(\frac{\pi}{4}\right) & 0 \\ -\sin\left(\frac{\pi}{4}\right)\cos\theta & \cos\left(\frac{\pi}{4}\right)\cos\theta & \sin\theta \\ \sin\left(\frac{\pi}{4}\right)\sin\theta & -\cos\left(\frac{\pi}{4}\right)\sin\theta & \cos\theta \end{bmatrix} \cdot \left(\begin{bmatrix} 0 \\ r_n \cos\phi \\ r_n \sin\phi \end{bmatrix}_{\text{Red}} + \begin{bmatrix} r_n \cos\phi \\ 0 \\ r_n \sin\phi \end{bmatrix}_{\text{Blue}} \right) \quad (3)$$

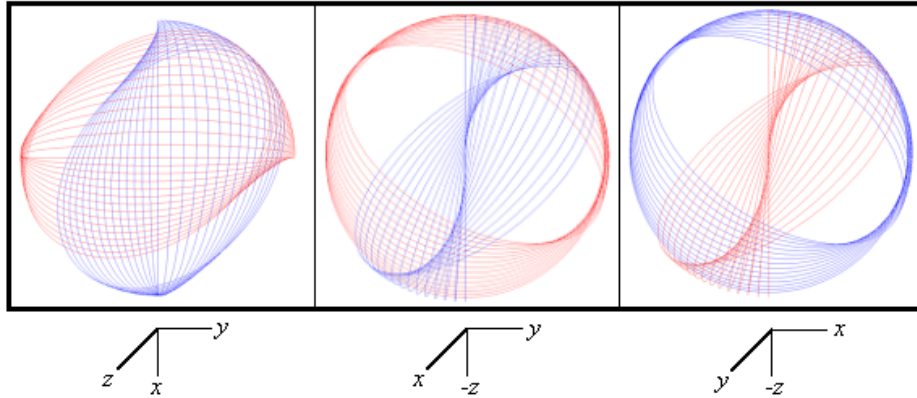
Substitution of the matrix given by Eq. (2) into Eq. (3) gives

$$\begin{bmatrix} x' \\ y' \\ z' \end{bmatrix} = \begin{bmatrix} \frac{1}{2} + \frac{\cos\theta}{2} & \frac{1}{2} - \frac{\cos\theta}{2} & -\frac{\sin\theta}{\sqrt{2}} \\ \frac{1}{2} - \frac{\cos\theta}{2} & \frac{1}{2} + \frac{\cos\theta}{2} & \frac{\sin\theta}{\sqrt{2}} \\ \frac{\sin\theta}{\sqrt{2}} & -\frac{\sin\theta}{\sqrt{2}} & \cos\theta \end{bmatrix} \cdot \left(\begin{bmatrix} 0 \\ r_n \cos\phi \\ r_n \sin\phi \end{bmatrix}_{\text{Red}} + \begin{bmatrix} r_n \cos\phi \\ 0 \\ r_n \sin\phi \end{bmatrix}_{\text{Blue}} \right) \quad (4)$$

$$\begin{bmatrix} x' \\ y' \\ z' \end{bmatrix} = \begin{bmatrix} \left(\left(\frac{1 - \cos \theta}{2} \right) r_n \cos \phi - \frac{\sin \theta}{\sqrt{2}} r_n \sin \phi \right)_{\text{Red}} + \left(\left(\frac{1 + \cos \theta}{2} \right) r_n \cos \phi - \frac{\sin \theta}{\sqrt{2}} r_n \sin \phi \right)_{\text{Blue}} \\ \left(\left(\frac{1 + \cos \theta}{2} \right) r_n \cos \phi + \frac{\sin \theta}{\sqrt{2}} r_n \sin \phi \right)_{\text{Red}} + \left(\left(\frac{1 - \cos \theta}{2} \right) r_n \cos \phi + \frac{\sin \theta}{\sqrt{2}} r_n \sin \phi \right)_{\text{Blue}} \\ \left(-\frac{\sin \theta}{\sqrt{2}} r_n \cos \phi + \cos \theta r_n \sin \phi \right)_{\text{Red}} + \left(\frac{\sin \theta}{\sqrt{2}} r_n \cos \phi + \cos \theta r_n \sin \phi \right)_{\text{Blue}} \end{bmatrix} \quad (5)$$

The RHCP photon-e&mvf that is generated by the rotation of the great-circle basis elements in the xz- and yz-planes about the $(\mathbf{i}_x, \mathbf{i}_y, 0\mathbf{i}_z)$ -axis by $\frac{\pi}{2}$ corresponding to the output of the matrix given by Eq. (5) is shown in Figure AV.2.

Figure AV.2. The field-line pattern given by Eq. (5) from three orthogonal perspectives of a RHCP photon-e&mvf corresponding to the first great circle magnetic field line and the second great circle electric field line shown with 6 degree increments of the angle θ . (Electric field lines red; Magnetic field lines blue).



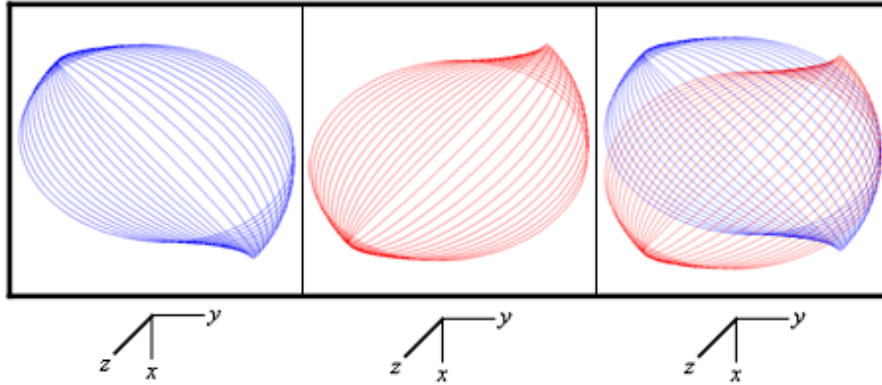
ANALYTICAL EQUATIONS TO GENERATE THE LEFT-HANDED CIRCULARLY POLARIZED PHOTON ELECTRIC AND MAGNETIC VECTOR FIELD BY ROTATION OF THE GREAT-CIRCLE BASIS ELEMENTS ABOUT THE $(\mathbf{i}_x, -\mathbf{i}_y, 0\mathbf{i}_z)$ -AXIS BY $\frac{\pi}{2}$

The left-handed circularly polarized (LHCP) photon electric and magnetic vector field (photon-e&mvf) is also generated following a similar procedure as that used to generate the orbitsphere in the Orbitsphere Equation of Motion for $\ell = 0$ Based on the Current Vector Field (CVF) section using the rotational matrices given therein. The LHCP photon-e&mvf is generated by the rotation of the basis elements comprising the great circle magnetic field line in the xz-plane and the great circle electric field line in the yz-plane about the $(\mathbf{i}_x, -\mathbf{i}_y, 0\mathbf{i}_z)$ -axis by $\frac{\pi}{2}$. A first transformation matrix is generated by the combined rotation of the great circles about the z-axis by $\frac{\pi}{4}$ then about the x-axis by θ where positive rotations about an axis are defined as clockwise:

$$\begin{bmatrix} x' \\ y' \\ z' \end{bmatrix} = \begin{bmatrix} \cos\left(\frac{\pi}{4}\right) & -\sin\left(\frac{\pi}{4}\right) & 0 \\ \sin\left(\frac{\pi}{4}\right)\cos\theta & \cos\left(\frac{\pi}{4}\right)\cos\theta & \sin\theta \\ -\sin\left(\frac{\pi}{4}\right)\sin\theta & -\cos\left(\frac{\pi}{4}\right)\sin\theta & \cos\theta \end{bmatrix} \cdot \left(\begin{bmatrix} 0 \\ r_n \cos\phi \\ r_n \sin\phi \end{bmatrix}_{\text{Red}} + \begin{bmatrix} r_n \cos\phi \\ 0 \\ r_n \sin\phi \end{bmatrix}_{\text{Blue}} \right) \quad (6)$$

The transformation matrix about $(\mathbf{i}_x, -\mathbf{i}_y, 0\mathbf{i}_z)$ is given by multiplication of the output of the matrix given by Eq. (6) by the matrix corresponding to a rotation about the z-axis of $\frac{\pi}{4}$. The output of the matrix given by Eq. (6) is shown in Figure AV.3 wherein θ is varied from 0 to $\frac{\pi}{2}$.

Figure AV.3. The electric, magnetic, and combined field-line pattern given by Eq. (6) from perspective of looking along the z-axis corresponding to the first great circle magnetic field line and the second great circle electric field line shown with 6 degree increments of the angle θ . (Electric field lines red; Magnetic field lines blue).



The rotation matrix about the z-axis by $\frac{\pi}{4}$, $R_z\left(\frac{\pi}{4}\right)$, is given by:

$$R_z\left(\frac{\pi}{4}\right) = \begin{bmatrix} \cos\left(\frac{\pi}{4}\right) & \sin\left(\frac{\pi}{4}\right) & 0 \\ -\sin\left(\frac{\pi}{4}\right) & \cos\left(\frac{\pi}{4}\right) & 0 \\ 0 & 0 & 1 \end{bmatrix} \quad (7)$$

Thus,

$$\begin{bmatrix} x' \\ y' \\ z' \end{bmatrix} = R_z\left(\frac{\pi}{4}\right) \cdot \begin{bmatrix} \cos\left(\frac{\pi}{4}\right) & -\sin\left(\frac{\pi}{4}\right) & 0 \\ \sin\left(\frac{\pi}{4}\right)\cos\theta & \cos\left(\frac{\pi}{4}\right)\cos\theta & \sin\theta \\ -\sin\left(\frac{\pi}{4}\right)\sin\theta & -\cos\left(\frac{\pi}{4}\right)\sin\theta & \cos\theta \end{bmatrix} \cdot \left(\begin{bmatrix} 0 \\ r_n \cos\phi \\ r_n \sin\phi \end{bmatrix}_{\text{Red}} + \begin{bmatrix} r_n \cos\phi \\ 0 \\ r_n \sin\phi \end{bmatrix}_{\text{Blue}} \right) \quad (8)$$

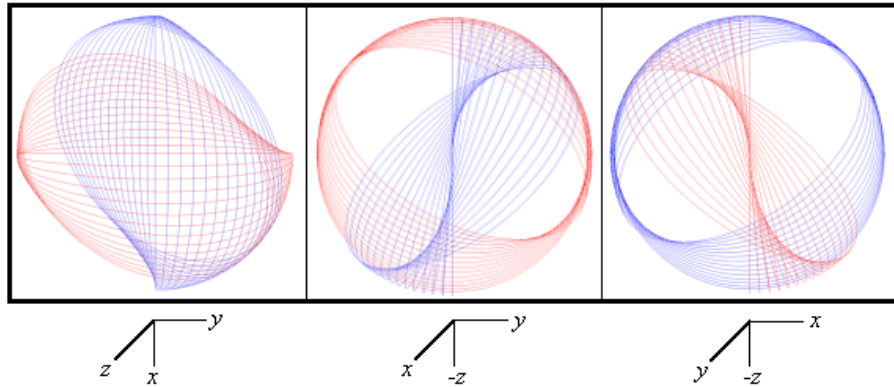
Substitution of the matrix given by Eq. (7) into Eq. (8) gives

$$\begin{bmatrix} x' \\ y' \\ z' \end{bmatrix} = \begin{bmatrix} \frac{1}{2} + \frac{\cos\theta}{2} & -\frac{1}{2} + \frac{\cos\theta}{2} & \frac{\sin\theta}{\sqrt{2}} \\ -\frac{1}{2} + \frac{\cos\theta}{2} & \frac{1}{2} + \frac{\cos\theta}{2} & \frac{\sin\theta}{\sqrt{2}} \\ -\frac{\sin\theta}{\sqrt{2}} & -\frac{\sin\theta}{\sqrt{2}} & \cos\theta \end{bmatrix} \cdot \left(\begin{bmatrix} 0 \\ r_n \cos\phi \\ r_n \sin\phi \end{bmatrix}_{\text{Red}} + \begin{bmatrix} r_n \cos\phi \\ 0 \\ r_n \sin\phi \end{bmatrix}_{\text{Blue}} \right) \quad (9)$$

$$\begin{bmatrix} x' \\ y' \\ z' \end{bmatrix} = \begin{bmatrix} \left(\left(-\frac{1}{2} + \frac{\cos\theta}{2} \right) r_n \cos\phi + \frac{\sin\theta}{\sqrt{2}} r_n \sin\phi \right)_{\text{Red}} + \left(\left(\frac{1}{2} + \frac{\cos\theta}{2} \right) r_n \cos\phi + \frac{\sin\theta}{\sqrt{2}} r_n \sin\phi \right)_{\text{Blue}} \\ \left(\left(\frac{1}{2} + \frac{\cos\theta}{2} \right) r_n \cos\phi + \frac{\sin\theta}{\sqrt{2}} r_n \sin\phi \right)_{\text{Red}} + \left(\left(-\frac{1}{2} + \frac{\cos\theta}{2} \right) r_n \cos\phi + \frac{\sin\theta}{\sqrt{2}} r_n \sin\phi \right)_{\text{Blue}} \\ \left(-\frac{\sin\theta}{\sqrt{2}} r_n \cos\phi + \cos\theta r_n \sin\phi \right)_{\text{Red}} + \left(-\frac{\sin\theta}{\sqrt{2}} r_n \cos\phi + \cos\theta r_n \sin\phi \right)_{\text{Blue}} \end{bmatrix} \quad (10)$$

The LHCP photon-e&mvf that is generated by the rotation of the great-circle basis elements in the xz- and yz-planes about the $(\mathbf{i}_x, -\mathbf{i}_y, 0\mathbf{i}_z)$ -axis by $\frac{\pi}{2}$ corresponding to the output of the matrix given by Eq. (10) is shown in Figure AV.4.

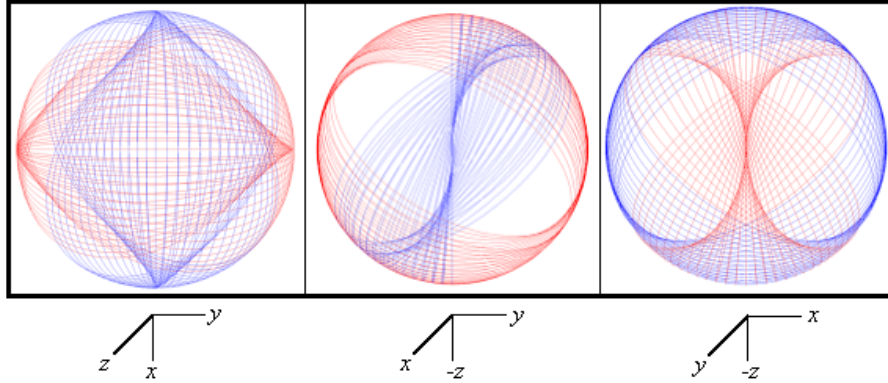
Figure AV.4. The field-line pattern given by Eq. (10) from three orthogonal perspectives of a LHCP photon-e&mvf corresponding to the first great circle magnetic field line and the second great circle electric field line shown with 6 degree increments of the angle θ . (Electric field lines red; Magnetic field lines blue).



GENERATION OF THE LINEARLY-POLARIZED PHOTON ELECTRIC AND MAGNETIC VECTOR FIELD

The linearly polarized (LP) photon-e&mvf is generated by the superposition of the RHCP photon-e&mvf and the LHCP photon-e&mvf as shown in Figure AV.5.

Figure AV.5. The field-line pattern given by Eqs. (5) and (10) from three orthogonal perspectives of a LP photon-e&mvf corresponding to the first great circle magnetic field line and the second great circle electric field line shown with 6 degree increments of the angle θ about each of the $(\mathbf{i}_x, \mathbf{i}_y, 0\mathbf{i}_z)$ - and $(\mathbf{i}_x, -\mathbf{i}_y, 0\mathbf{i}_z)$ -axes. (Electric field lines red; Magnetic field lines blue).



PHOTON FIELDS IN THE LABORATORY FRAME

Since the power flow, \mathbf{P} , is governed by the Poynting power theorem given by

$$\mathbf{P} = \nabla \cdot (\mathbf{E} \times \mathbf{H}) \quad (11)$$

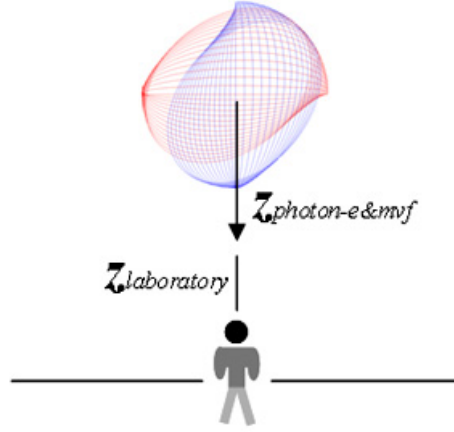
and the time-averaged angular momentum density is given by Eq. (4.1), $\mathbf{m} = \int \frac{1}{8\pi c} \text{Re}[\mathbf{r} \times (\mathbf{E} \times \mathbf{B}^*)] dx^4 = \hbar$, it is apparent that the photon propagation axis is along the $\mathbf{E} \times \mathbf{H}$ -vector at the intersection point of the basis elements, the orthogonal great-circle electric and magnetic field lines. Consider the RHCP photon-e&mvf. The primary intersection occurs at the z-axis of the stationary xyz-coordinate system. This point is also the initial position of the z'-axis of the x'y'z'-coordinate system that is rotated about the $(\mathbf{i}_x, \mathbf{i}_y, 0\mathbf{i}_z)$ -axis by $\frac{\pi}{2}$ wherein the great-circle field lines are stationary with respect to this system. Then, the z' and -z'-intersection of the two orthogonal great-circle field lines move along a great circle in the first and third quadrants, respectively, of a plane that is parallel with the z-and $(-\mathbf{i}_x, \mathbf{i}_y, 0\mathbf{i}_z)$ -axes as the photon-e&mvf is generated. Consequently, the $\mathbf{E} \times \mathbf{H}$ -vector is orthogonal to the $\frac{\pi}{2}$ -rotational axis, the $(\mathbf{i}_x, \mathbf{i}_y, 0\mathbf{i}_z)$ -axis.

Consider an observer at the origin of his frame with the photon propagating at light-speed c along the z-axis relative to the observer as shown in Figure AV.6. The geometrical cross section of the photon changes as a function of its distance from the origin as it passes the observer. The differential length s on a spherical surface of radius r_0 is given by

$$s = r_0 \sin \theta d\theta \quad (12)$$

where θ is the same parameter as the rotational angle to generate the photon-e&mvf. Thus, the differential length of the great-circle field lines has a $\sin \theta$ geometrical dependence relative to the observer. In addition, due to special relativity the $\mathbf{E} \times \mathbf{H}$ -vector of the photon-e&mvf has an angular dependence in its frame that is different from that of the observer in his laboratory frame. The transform is given by considering total field invariance under Gauss' integral law.

Figure AV.6. An observer at the origin of his frame with the photon-e&mvf stationary in its own frame propagating at light-speed c relative to the observer along its z-axis ($z_{\text{photon-e\&mvf}}$) that is collinear to the z-axis of the observer, $z_{\text{laboratory}}$.



As shown in the Fields Based on Invariance Under Gauss' Integral Law section, this law requires that the electric and magnetic field lines are perpendicular to the direction of power flow, the direction of propagation, being the z-axis. The electric and magnetic fields on the spherical surface of the photon-e&mvf are perpendicular at the z-axis and the projection of the fields into a plane perpendicular to the z-axis has a $\cos \theta$ dependence which is the equivalent to the dot product of the z'-axis ($\mathbf{E} \times \mathbf{H}$ - axis) with the z-axis wherein θ is the same parameter as the rotational angle to generate the photon-e&mvf. The fields are each then given as this projection of the great circle basis element transverse to the z-axis times the differential length of the spherical surface along the z-axis given by Eq. (12). Thus, the electric field \mathbf{E} is given by

$$\mathbf{E} = E_0 \cos \theta \sin \theta \mathbf{i}_z \times \mathbf{i}_z \quad (13)$$

where E_0 is a constant. Using a trigonometric identity

$$\cos \theta \sin \theta = \frac{1}{2} \sin 2\theta \quad (14)$$

gives

$$\mathbf{E} = \frac{E_0}{2} \sin 2\theta \mathbf{i}_z \times \mathbf{i}_z \quad (15)$$

Since the magnetic field is perpendicular to the electric field according to Maxwell's equations (Eqs. (4.2-4.3)), Eq. (4.10) follows from Eq. (15), and the magnetic field \mathbf{H} is given by

$$\mathbf{H} = \sqrt{\frac{\epsilon_0}{\mu_0}} \frac{E_0}{2} \sin 2\theta \mathbf{i}_z \times (\mathbf{i}_z \times \mathbf{i}_z) \quad (16)$$

The natural coordinates for the photon-e&mvf are cylindrical wherein the electric and magnetic field lines make a helical trajectory relative to an observer who is passed at the light speed. The transverse-plane-projected electric and magnetic fields rotate about the z-axis over a 2π angular span of the arguments of Eqs. (15) and (16) corresponding to the π span along the z-axis from the $\frac{\pi}{2}$ rotation of the two orthogonal great circle field lines about the $(\mathbf{i}_x, \mathbf{i}_y, 0\mathbf{i}_z)$ -axis to generate the photon-e&mvf.

The rotation about the z-axis requires that the photon angular momentum is along the z-axis. Using the time-averaged angular momentum density give by Eq. (4.1), the direction of $\mathbf{E} \times \mathbf{B}^*$ is the z-axis, and the vector rotates at angular frequency ω about the z-axis in the direction of \mathbf{i}_ϕ . Thus, the corresponding time-averaged integral of the unit-vector cross products of Eq. (4.1) is given by

$$\mathbf{i}_\rho \times \mathbf{i}_\phi = \mathbf{i}_z \quad (17)$$

Eq. (4.10) follows from the electric and magnetic fields that rotate time harmonically transverse to and about the z-axis according to the time function $k(t)$ given by

$$k(t) = e^{-j\omega t} \quad (18)$$

For example, the spatial distribution of the fields of a right-handed circularly polarized photon-e&mvf in the laboratory frame is shown in Figures 4.5 and 4.6. More specifically, Figure AV.7a and b show the visualization of the fields in the laboratory frame for the observer shown in Figure AV.6.

Figure AV.7. The electric (red) and magnetic (blue) field lines of a right-handed circularly polarized photon-e&mvf as seen along the axis of propagation in the lab inertial reference frame as it passes a fixed point. (a) Three-dimension view. (b). Two-dimensional view.

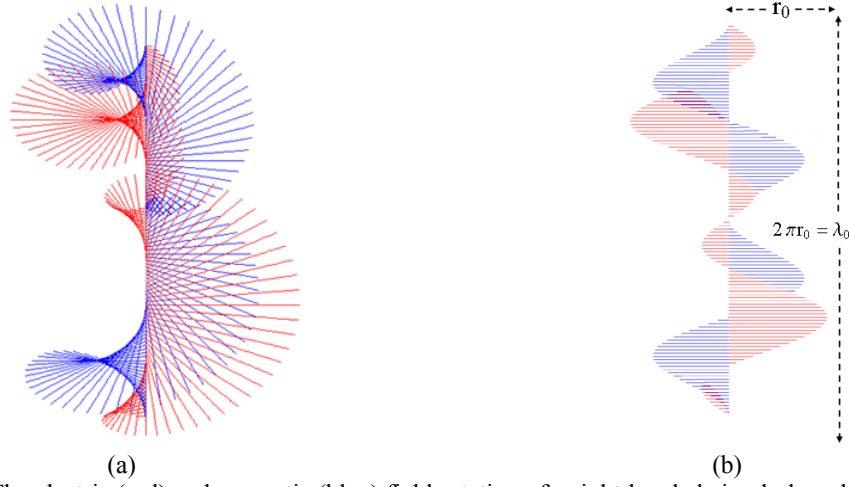
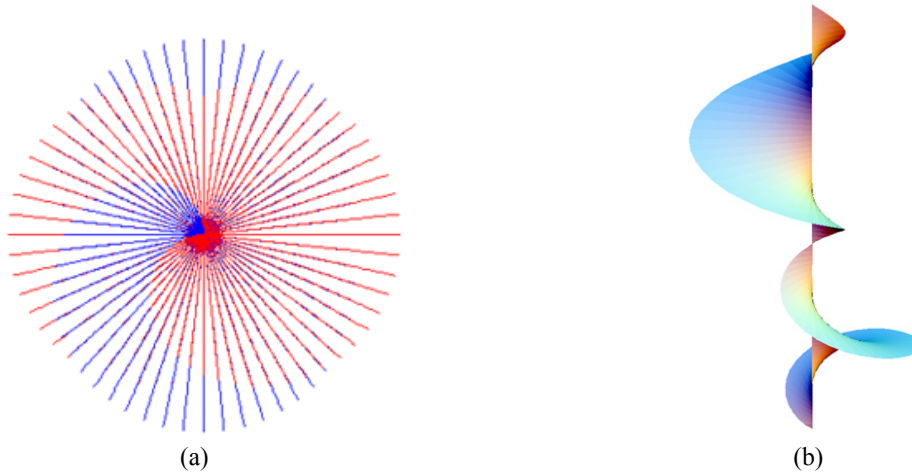


Figure AV.8. (a) The electric (red) and magnetic (blue) field rotation of a right-handed circularly polarized photon-e&mvf as seen transverse to the axis of propagation in the lab inertial reference frame as it passes a fixed point. (b) A surface rendering of the electric field lines of a right-handed circularly polarized photon-e&mvf as seen along the axis of propagation in the lab inertial reference frame as it passes a fixed point



The corresponding photon-e&mvf equation in the lab frame is

$$\mathbf{E} = E_0 [\mathbf{x} - i\mathbf{y}] e^{-jk_z z} e^{-j\omega t} \quad (19)$$

$$\mathbf{H} = \left(\frac{E_0}{\eta} \right) [\mathbf{y} - i\mathbf{x}] e^{-jk_z z} e^{-j\omega t} = E_0 \sqrt{\frac{\epsilon}{\mu}} [\mathbf{y} - i\mathbf{x}] e^{-jk_z z} e^{-j\omega t} \quad (20)$$

with a wavelength of

$$\lambda = 2\pi \frac{c}{\omega} \quad (21)$$

The relationship between the photon orbitsphere radius and wavelength is

$$2\pi r_0 = \lambda_0 \quad (22)$$

Using Eqs. (4.1), and (15-18) with

$$\rho = r_0 \sin \theta \quad (23)$$

the electric and magnetic-field parameter E_0 can be solved:

$$\frac{1}{8\pi c} \int_0^{\frac{2\pi}{\omega}} \int_0^{2\pi} \int_0^{\pi} \int_0^{\infty} r \sin \theta \sqrt{\frac{\epsilon_0}{\mu_0}} \frac{E_0^2}{4} \sin^2 2\theta \sin^2 \omega t r^2 \delta(r - r_0) \sin \theta dr d\theta d\phi dt = \hbar \quad (24)$$

where Eq. (4.1) was converted to MKS units. The integration over the period and the surface gives

$$\frac{1}{8\pi c} \sqrt{\frac{\epsilon_0}{\mu_0}} \frac{E_0^2}{4} \frac{2\pi}{2\omega} 2\pi r_0^3 \int_0^\pi \sin^2 2\theta \sin^2 \theta d\theta = \hbar \quad (25)$$

$$\sqrt{\frac{\epsilon_0}{\mu_0}} \frac{E_0^2}{32c} \frac{2\pi}{\omega} r_0^3 \int_0^\pi \sin^2 2\theta \left(\frac{1 - \cos 2\theta}{2} \right) d\theta = \hbar \quad (26)$$

Using the wave equation relationship and the relationship between the wavelength and the radius of the photon-e&mvf given by Eq. (21) and Eq. (22), respectively, with the integral by Lide [1] gives

$$\sqrt{\frac{\epsilon_0}{\mu_0}} \frac{E_0^2}{32} \frac{\pi}{\omega^4} c^2 \left(\left(\frac{\theta}{2} - \frac{1}{8} \sin 4\theta \right)_0^\pi - \int_0^\pi \sin^2 2\theta \cos 2\theta d\theta \right) = \hbar \quad (27)$$

The second integral by Lide [1] gives

$$\sqrt{\frac{\epsilon_0}{\mu_0}} \frac{E_0^2}{32} \frac{\pi}{\omega^4} \frac{c}{\sqrt{\epsilon_0 \mu_0}} c \left(\frac{\pi}{2} - \left(\frac{\sin^3 2\theta}{3\theta} \right)_0^\pi \right) = \hbar \quad (28)$$

$$\frac{E_0^2}{64} \frac{\pi^2}{\omega^4 \mu_0} c = \hbar \quad (29)$$

Thus,

$$E_0 = \sqrt{\frac{64\omega^4 \mu_0 \hbar}{c\pi^2}} = \frac{8\omega^2}{\pi} \sqrt{\frac{\mu_0 \hbar}{c}} \quad (30)$$

which has the required MKS units of Vm^{-1} . The photon-e&mvf travels rectilinearly in the laboratory frame at light speed. Due to the total-field invariance under Gauss' integral law, E_0 is greater in the laboratory frame than in the photon-e&mvf frame.

The correction γ^* is given by Eq. (1.293). Thus, E_0 in the laboratory frame is given by

$$E_0 = \gamma^* \frac{8\omega^2}{\pi} \sqrt{\frac{\mu_0 \hbar}{c}} = 2\pi \frac{8\omega^2}{\pi} \sqrt{\frac{\mu_0 \hbar}{c}} = 16\omega^2 \sqrt{\frac{\mu_0 \hbar}{c}} \quad (31)$$

REFERENCE

1. D. R. Lide, *CRC Handbook of Chemistry and Physics*, 79th Edition, CRC Press, Boca Raton, Florida, (1998-9), pp. A-38; A-40.

